The Influence of Oil Contamination on Flow Control Valve Operation

DOMAGALA Mariusz[1,a *], MOMENI Hassan[2,b]
and FABIS-DOMAGALA Joanna[1,c]

[1] Cracow University of Technology, Faculty of Mechanical Engineering, Al. Jana Pawla II 37
31-841 Cracow, Poland

[2] Department of Mechanical and Marine Engineering, Western Norway University of Applied Sciences, N5020 Bergen, Norway

[a]mariusz.domagala@pk.edu.pl, [b] Hassan.Momeni@hvl.no, [c] joanna.fabis-domagala@pk.edu.

Keywords: Flow Control Valve, Solid Particle Simulation, CFD Simulation

Abstract. This study presents CFD simulations of the flow of contaminated oil inside a control valve to investigate the influence of solid contaminants on the valve operational features. The Euler-Lagrange approach has been used to simulate the flow of oil contaminated with solid particles. The CFD simulations allowed determining the effect of solid contamination on the value of hydrodynamic force and a pressure drop for different contamination levels and valve opening.

Introduction

Fluid power systems are widely used in industrial applications due to their high power density, dynamic load dissipation possibilities and flexibility unattainable for other systems. They use pressure energy created by pumps, which further transfers accumulated energy to receivers. Fluid power systems have been used for decades and use hydro-mechanical components, which are often complemented with electronic control systems recently, making them still competitive among other drive systems. The complexity level of fluid power systems depends on realized tasks and may include from a few to hundreds of components. Despite the undoubted progress in fluid power systems reliability, some problems are still not solved and are objects of many recent studies. One of the main problems of these systems is the contamination of working fluid, which is recognized as a leading cause of failures [1, 2]. The recent efforts in preventing hydraulic systems against the negative influence of contaminants is mainly focused on monitoring contamination levels [3, 4]. However, the practice shows that fully prevention of hydraulic fluid against contamination is nearly impossible even by using sophisticated filtration systems. Contaminants might have different natures and sources. They can occur due to wear or ingression (solid particles) or effects of chemical agents (air and water). One of the primary contamination sources is the one generated by the hydraulic system during normal operation due to wear, erosion or corrosion. The component recognized as the primary source of solid (metal) contaminants are pumps, where relative motion and high structural load may intensify factors responsible for wear, erosion, cavitation or fatigue. In particular, the vane pumps are found to be the significant sources of oil contamination, and industrial standards use them as a reference component for testing oil contamination levels [5-7].

During operation, the solid contaminants gather momentum from working fluid and may affect surfaces, causing their erosion, what may lead to failure, malfunction or reduce the lifetime of critical components of the system. Such components are valves, which malfunction or failures may lead to severe damages and catastrophic events. The wear caused by solid contaminants on valves can be evaluated by experimental tests or numerical simulations in which computational fluid dynamics (CFD) tools are implemented [8, 9]. As the contamination of working fluid is inevitable, the industrial standards [10] defines the cleanliness class of fluid as a rate of particle size in specified oil capacity.

The failure or wear caused by solid contaminants is a long term process, and symptoms can be relatively easy to identify. However, their influence on the operational characteristics of crucial components of fluid power systems is unknown. This study attempts to evaluate oil contamination on flow control valve functional features achieved by implementing the Euler-Lagrange flow simulation approach.

The obtained results may be useful both for researchers using similar modeling methods [11-14] and industries with machines and devices equipped with valve hydraulics, such as biotechnological engineering [15], wastewater treatment [16, 17], and internal combustion engine accessories [18]. It should also be a guideline for the use of special coatings [19, 20], including modified ones [21, 22] in similar situations, to avoid disfunction. The schema of analysis itself can be inspiring both for similar modeling techniques [23-25] and for production management systems [26] and quality management systems [27-30].

Methodology

The flow simulation of fluid with solid particles has been performed by Euler-Lagrange multiphase flow in which hydraulic oil is considered as continuous Euler phase while particles as Lagrange phase. The CFD method employs RANS (Reynolds Averaged Navier-Stokes) equations which define scalars as mean values and fluctuations over this value. RANS defines fluid velocity as:

$$u_i = \overline{u}_i + u_i' \tag{1}$$

where: $\overline{u}_i$ – is the mean velocity, u_i' – is the fluctuating velocity, i – stands for velocity component.

Thus the RANS equations have the following form:

$$\frac{\partial \rho}{\partial t} + \frac{\partial \rho}{\partial x_i}(\rho u_i) = 0 \tag{2}$$

$$\frac{\partial \rho}{\partial t}(\rho u_i) + \frac{\partial \rho}{\partial x_j}(\rho u_i u_j) = -\frac{\partial p}{\partial x_i} + \frac{\partial}{\partial x_j}\left[\mu\left(\frac{\partial u_i}{\partial x_j} + \frac{\partial u_j}{\partial x_i} - \frac{2}{3}\delta_{ij}\frac{\partial u_i}{\partial x_i}\right)\right] + \frac{\partial}{\partial x_j}\left(-\rho\overline{u_\imath u_j}\right) \tag{3}$$

where: ρ – is the fluid density, u – is the fluid velocity, p – is pressure, μ – is the dynamic viscosity, δ – is the Kronecker function.

The term $-\rho\overline{u_\imath u_j}$ represents the effects of turbulence (Reynolds stress) and makes the set of Eq. (2) and Eq. (3) to be open. The RANS equations can be closed by the use of the Boussinesq hypothesis:

$$-\rho\overline{u_\imath u_j} = \mu_t\left(\frac{\partial u_i}{\partial x_j} + \frac{\partial u_j}{\partial x_i}\right) - \frac{2}{3}\delta_{ij}\left(\rho k + \mu_t\frac{\partial u_k}{\partial x_k}\right) \tag{4}$$

and employing the turbulence model.

Solid particles are represented as discreet phases and are tracked into the fluid domain during fluid flow. The equation of motion for a single particle according to Basset, Boussinesq and Oseen is as follows:

$$m_p \frac{dU_p}{dt} = F_D + F_B + F_R + F_{VM} + F_P + F_{BA} \quad (5)$$

where: F_D – drag force, F_B – buoyancy force, F_R – Coriolis force, F_{VM} is inertia force of fluid occupied by a particle (Virtual Mass), F_P – pressure force, F_{BA} – Basset force

The following equation expresses the inertia force of fluid occupied by a particle (Virtual Mass):

$$F_{VM} = \frac{C_{VM}}{2} m_F \left(\frac{dU_F}{dt} - \frac{dU_P}{dt}\right) \quad (6)$$

Combining Eq. 5 and Eq. 6, we have:

$$\frac{dU_p}{dt} = \left(\frac{1}{m_p + \frac{C_{VM}}{2} m_F}\right)(F_D + F_B + F_R + F'_{VM} + F_P + F_{BA}) \quad (7)$$

where:

$$F'_{VM} = \frac{C_{VM}}{2} m_F (U_F \nabla U_F) \quad (8)$$

$m_P = \frac{\pi}{6} d_P^3 \rho_P$ is particle mass, $m_F = \frac{\pi}{6} d_P^3 \rho_F$ is fluid mass, d_p is the particle diameter, ρ_P, ρ_F is the density of particle and fluid, respectively.

Introducing R_{VM} as:

$$R_{VM} = \frac{m_P}{m_P + \frac{C_{VM}}{2} m_F} = \frac{\rho_P}{\rho_P + \frac{C_{VM}}{2} \rho_F} \quad (9)$$

we will get Eq. 5 in the following form:

$$\frac{dU_p}{dt} = \left(\frac{R_{VM}}{m_p}\right)(F_D + F_B + F_R + F'_{VM} + F_P + F_{BA}) \quad (10)$$

Case Study

The valve presented in Fig. 1 is a proportional solenoid controlled flow control valve whose primary purpose is to maintain a constant flow rate independently on a pressure difference between the valve supply and receiver lines.

The valve consists of two spools (2,3) assembled in the body (1) inside the sleeve (4). The value of flow rate is controlled by a solenoid, which directly acts on the spool (3). The position of the second spool (2) depends on the pressure at the entry flow ducts (valve supply line) and outlet flow ducts (receiver line) and is determined by the force balance on the spool (2). Hydrodynamic reactions are among those forces that play the leading role in valve proper operation.

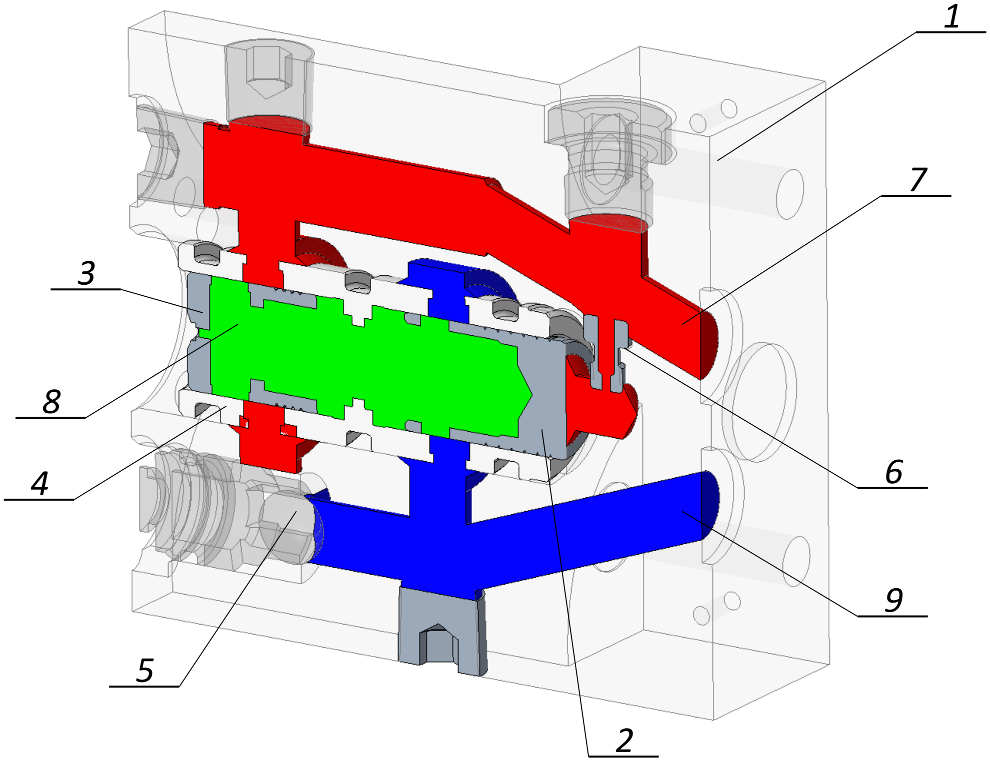

Fig. 1. *Flow control valve: 1 – valve body, 2,3 – spools, 4 – sleeve, 5 – non return valve, 6 – nozzle, 7 – entry flow ducts, 8 – flow duct inside spools, 9 – outlet flow duct.*

CFD Simulation

The main purpose of CFD simulation was to evaluate flow forces and pressure drops during the flow of contaminated oil inside the valve. The simulation was conducted with Euler-Lagrange approach in Ansys CFX code for both spools fixed position and steady state conditions. The following assumptions have been used:

Continous phase:

- fluid (hydraulic oil) has a constant properties: density 880 [kg/m^3], viscosity υ=40 [mm^2/s];
- flow is turbulent: the k-ϖ turbulence has been applied;
- heat transfer is neglected;
- cell type: hybrid, tetrahedral with prism.

Lagrangian phase:

- particles have spheres shape with a diameter of 1 [µm] and constant properties (steel), with 2.5% and 5% of fluid mass flow rate;
- interaction between particles and fluid is fully coupled;
- particles are uniformly injected over the valve inlet.

CFD model is presented in Fig. 2. The grid in gaps in which fluids flow has been refined to increase simulation accuracy. Due to the symmetry of flow ducts, half of the geometry was used, and symmetry boundary condition has been applied.

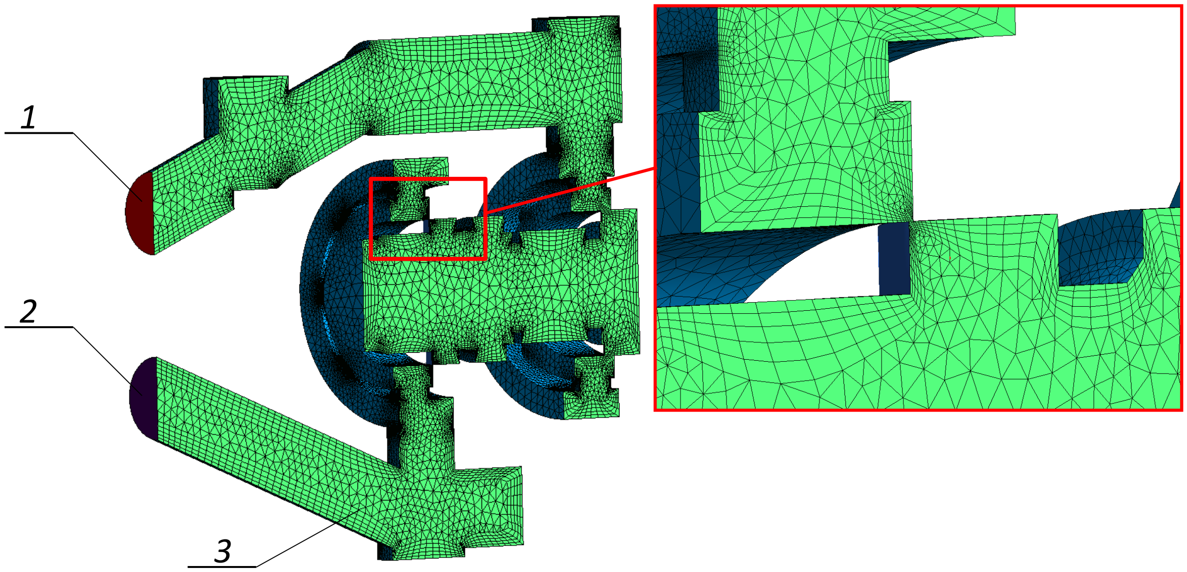

Fig. 2. *CFD model: 1 – inlet, 2 – outlet,3-symmetry plane.*

Numerical simulation has been performed for constant mass flow rate with a different contribution of solid contaminants. Two oil contamination levels have been checked: 4000 and 8000 particles per 1 [ml], which gives approximately 2.5% and 5% mass flow rates, respectively. It has to be mentioned that particle size used in the simulation, if far below the minimal value, is recognized as a contaminant by the relevant standard [10] and equals 4 [μm]. Results of CFD simulation have been presented in Fig. 3 as a fluid velocity on the symmetry plane and solid particle tracks and velocity.

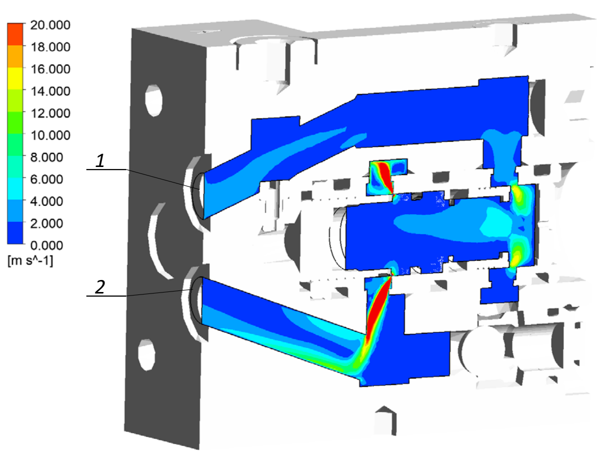

Fig. 3a. *Fluid velocity at normalized opening 0.1 in [m/s], 1 – inlet, 2 – outlet*

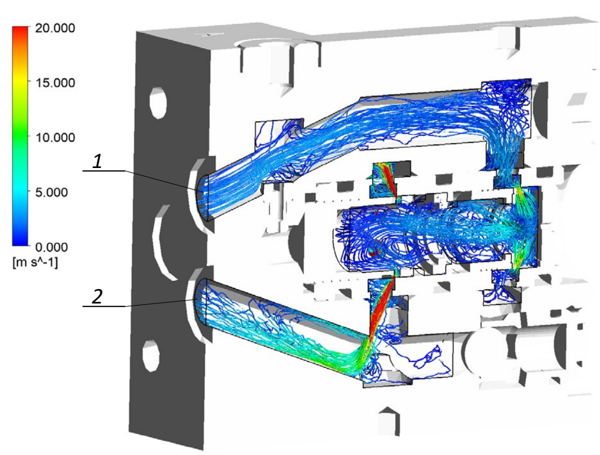

Fig. 3b. *Solid particle tracks at normalized opening 0.1 in [m/s], 1 – inlet, 2 – outlet*

The simulations have been performed for the constant flow rate (15 dm^3/min) and fixed position of spools (2,3). Figure 4 shows the value of the hydrodynamic force (flow force) on the spool (2) and total pressure drop for different spool (2) positions (valve opening).

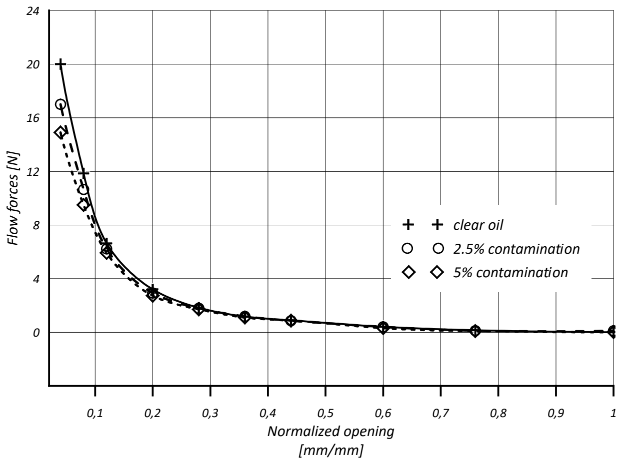

Fig. 4a. *Flow forces on the spool (3) for constant flow rate of 15 [dm^3/min].*

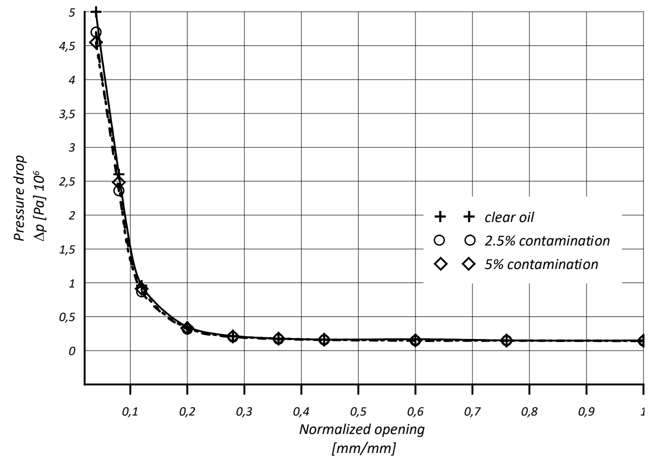

Fig. 4b. *Pressure drop for a constant flow rate of 15 [dm^3/min].*

The above results indicate that solid contaminants affect the hydrodynamic force for small valve openings (up to 0.15) while differences are almost undistinguishable for larger openings. Less than minor pressure drop differences were recorded even for small valve openings.

Summary

Protection of hydraulic oil in fluid power systems against contamination is almost impossible in a real world application. Therefore, this study attempts to evaluate the influence of the level of solid contamination on the flow control valve feature, which is critical for valve operation. The proposed method uses computational fluid dynamics (CFD) tools and Euler-Lagrange approach to simulate contaminated fluid flow inside the flow control valve. The simulations have been conducted for two different contamination levels. The working fluid included metal particles. Obtained results show that the presented contamination levels (2.5% and 5% of fluid mass flow rate) affect flow forces while pressure drop changes are almost negligible. However, it has to be added that presented results correspond to the idealized situation in which metal particles have a uniform shape and size. In real world applications, the particle size and distribution may strongly depend on system complexity, implemented components or even working conditions. Despite this, the CFD tools seem to be effective for investigating solid particles' influence on fluid power components.

References

[1] S. Li, Z. Yang, H. Tian, C. Chen, Y. Zhu, S. Lu. Failure Analysis for Hydraulic System of Heavy-Duty Machine Tool with Incomplete Failure Data. Appl. Sci. 14 (2021) art. 1249. https://doi.org/10.3390/app11031249

[2] J. Fabis-Domagala, M. Domagala, H. Momeni. A Concept of Risk Prioritization in FMEA Analysis for Fluid Power Systems. Energies 14 (2021) art. 6482. https://doi.org/10.3390/en14206482

[3] L. Zeng, Z. Yu, H. Zhang, X. Zhang, H. Chen. A high sensitive multi-parameter micro sensor for the detection of multi-contamination in hydraulic oil, Sensors and Actuators A: Physical 282 (2018) 197-205. https://doi.org/10.1016/j.sna.2018.09.023.

[4] F. Ng, J.A. Harding, J. Glass. Improving hydraulic excavator performance through in line hydraulic oil contamination monitoring, Mech. Systems and Signal Process. 83 (2017) 176-193. https://doi.org/10.1016/j.ymssp.2016.06.006.

[5] ISO 20763:2004. Petroleum and Related Products—Determination of Anti-Wear Properties of Hydraulic Fluids—Vane Pump Method; International Organization for Standardization: Geneva, Switzerland, 2004

[6] DIN 51389-1. Determination of Lubricants; Mechanical Testing of Hydraulic Fluids in the Vane-Cell-Pump; General Working Principles; DIN Deutsches Institut für Normung e. V.: Berlin, Germany, 1982

[7] ASTM D7043-17. Standard Test Method for Indicating Wear Characteristics of Non-Petroleum and Petroleum Hydraulic Fluids in a Constant Volume Vane Pump; ASTM International: West Conshohocken, PA, USA, 2017

[8] M. Domagala, H. Momeni, J. Fabis-Domagala, G. Filo, M. Krawczyk, J. Rajda. Simulation of Particle Erosion in a Hydraulic Valve, Materials Research Proceedings 5 (2018) 17-24. https://dx.doi.org/10.21741/9781945291814-4

[9] Y. Yaobao, Y. Jiayang, G. Shengrong. Numerical study of solid particle erosion in hydraulic spool valves, Wear 392-393 (2017) 147-189. https://doi.org/10.1016/j.wear.2017.09.021

[10] ISO 4406: Hydraulic fluid power — Fluids — Method for coding the level of contamination by solid particles, International Organization for Standardization: Geneva, Switzerland, 2021

[11] M. Zmindak, L. Radziszewski, Z. Pelagic, M. Falat. FEM/BEM techniques for modelling of local fields in contact mechanics, Communications - Scientific Letters of the University of Zilina 17 (2015) 37-46.

[12] T. Lipiński. Corrosion resistance of 1.4362 steel in boiling 65% nitric acid, Manufacturing Technology 16 (2016) 1004-1009.

[13] Ł.J. Orman Ł.J., N. Radek, J. Pietraszek, M. Szczepaniak. Analysis of enhanced pool boiling heat transfer on laser-textured surfaces. Energies 13 (2020) art. 2700. https://doi.org/10.3390/en13112700

[14] E. Lisowski, J. Rajda, G. Filo, P. Lempa. Flow Analysis of a 2URED6C Cartridge Valve, Lecture Notes in Mechanical Engineering 24 (2021) 40-49. https://doi.org/10.1007/978-3-030-59509-8_4

[15] E. Skrzypczak-Pietraszek. Phytochemistry and biotechnology approaches of the genus Exacum. In: The Gentianaceae - Volume 2: Biotechnology and Applications, 2015, 383-401. https://doi.org/10.1007/978-3-642-54102-5_16

[16] M. Zenkiewicz, T. Zuk, J. Pietraszek, P. Rytlewski, K. Moraczewski, M. Stepczyńska. Electrostatic separation of binary mixtures of some biodegradable polymers and poly(vinyl chloride) or poly(ethylene terephthalate), Polimery/Polymers 61 (2016) 835-843. https://doi.org/10.14314/polimery.2016.835

[17] E. Radzyminska-Lenarcik, R. Ulewicz, M. Ulewicz. Zinc recovery from model and waste solutions using polymer inclusion membranes (PIMs) with 1-octyl-4-methylimidazole, Desalination and Water Treatment 102 (2018) 211-219. https://doi.org/10.5004/dwt.2018.21826

[18] M. Kekez, L. Radziszewski, A. Sapietova. Fuel type recognition by classifiers developed with computational intelligence methods using combustion pressure data and the crankshaft angle at which heat release reaches its maximum, Procedia Engineering 136 (2016) 353-358. https://doi.org/10.1016/j.proeng.2016.01.222

[19] A. Dudek, R. Wlodarczyk. Structure and properties of bioceramics layers used for implant coatings, Solid State Phenom. 165 (2010) 31-36. https://doi.org/10.4028/www.scientific.net/SSP.165.31

[20] N. Radek, J. Pietraszek, A. Gadek-Moszczak, Ł.J. Orman, A. Szczotok. The morphology and mechanical properties of ESD coatings before and after laser beam machining, Materials 13 (2020) art. 2331. https://doi.org/10.3390/ma13102331

[21] N. Radek, J. Pietraszek, A. Goroshko. The impact of laser welding parameters on the mechanical properties of the weld, AIP Conf. Proc. 2017 (2018) art.20025. https://doi.org/10.1063/1.5056288

[22] N. Radek, J. Konstanty, J. Pietraszek, Ł.J. Orman, M. Szczepaniak, D. Przestacki. The effect of laser beam processing on the properties of WC-Co coatings deposited on steel. Materials 14 (2021) art. 538. https://doi.org/10.3390/ma14030538

[23] J. Pietraszek, A. Gadek-Moszczak, N. Radek. The estimation of accuracy for the neural network approximation in the case of sintered metal properties. Studies in Computational Intelligence 513 (2014) 125-134. https://doi.org/10.1007/978-3-319-01787-7_12

[24] J. Pietraszek, E. Skrzypczak-Pietraszek. The uncertainty and robustness of the principal component analysis as a tool for the dimensionality reduction. Solid State Phenom. 235 (2015) 1-8. https://doi.org/10.4028/www.scientific.net/SSP.235.1

[25] J. Pietraszek, R. Dwornicka, A. Szczotok. The bootstrap approach to the statistical significance of parameters in the fixed effects model. ECCOMAS 2016 – Proc. 7th European Congress on Computational Methods in Applied Sciences and Engineering 3, 6061-6068. https://doi.org/10.7712/100016.2240.9206

[26] A. Maszke, R. Dwornicka, R. Ulewicz. Problems in the implementation of the lean concept at a steel works – Case study, MATEC Web of Conf. 183 (2018) art.01014. https://doi.org/10.1051/matecconf/201818301014

[27] T. Styrylska, J. Pietraszek. Numerical modeling of non-steady-state temperature-fields with supplementary data. Zeitschrift fur Angewandte Mathematik und Mechanik 72 (1992) T537-T539.

[28] J. Pietraszek. Response surface methodology at irregular grids based on Voronoi scheme with neural network approximator. 6th Int. Conf. on Neural Networks and Soft Computing JUN 11-15, 2002, Springer, 250-255. https://doi.org/10.1007/978-3-7908-1902-1_35

[29] J. Pietraszek, N. Radek, A.V. Goroshko. Challenges for the DOE methodology related to the introduction of Industry 4.0. Production Engineering Archives 26 (2020) 190-194. https://doi.org/10.30657/pea.2020.26.33

[30] D. Siwiec, R. Dwornicka, A. Pacana. Improving the non-destructive test by initiating the quality management techniques on an example of the turbine nozzle outlet, Materials Research Proceedings 17 (2020) 16-22. https://doi.org/10.21741/9781644901038-3